Interaction of the Fibronectin COOH-Terminal Fib-2 Regions with Fibrin: Further Characterization and Localization of the Fib-2-Binding Sites†

Evgeny Makogonenko,‡ Kenneth C. Ingham,§ and Leonid Medved*,‡

Center for Vascular and Inflammatory Diseases and the Department of Biochemistry and Molecular Biology, University of Maryland School of Medicine, Baltimore, Maryland 21201, and Department of Biochemistry and Molecular Biology, the George Washington University School of Medicine and Health Sciences, Washington, D.C. 20037

Received January 23, 2007; Revised Manuscript Received March 8, 2007

ABSTRACT: Incorporation of fibronectin into fibrin clots is important for the formation of a provisional matrix that promotes cell adhesion and migration during wound healing. Previous studies revealed that this incorporation occurs through noncovalent interaction between two NH_2-terminal Fib-1 regions of fibronectin (one on each chain) and the αC-regions of fibrin, and is further reinforced by factor XIIIa-mediated covalent cross-linking of fibronectin to the fibrin matrix. To clarify the role of another pair of fibrin-binding regions, Fib-2, located at the disulfide-linked COOH-terminal ends of fibronectin, we prepared by limited proteolysis a dimeric 140 kDa $(Fib\text{-}2)_2$ fragment containing both Fib-2 regions and tested its interaction with recombinant fragments corresponding to the αC regions of fibrin(ogen). In both ELISA and surface plasmon resonance (SPR) experiments 140 kDa $(Fib\text{-}2)_2$ bound to the immobilized Aα221−610 αC-fragment. However, the affinity of binding was substantially lower than that for Fib-1. Ligand blotting and ELISA established that the Fib-2 binding site is located in the connector part of the αC region including residues Aα221−391. Analysis of the SPR-detected binding of fibronectin to the immobilized Aα221−610 αC-fragment revealed two types of fibronectin-binding sites, one with high affinity and another one with much lower affinity. Competition experiments revealed about 30% inhibition of the Fib-2 mediated binding by increasing concentrations of Fib-1 fragment suggesting partial overlap of the two sets of binding sites. Based on these results and our previous studies we propose a mechanism of interaction of fibronectin with fibrin in which both Fib-1 and Fib-2 play a role.

Fibrinogen is a blood clotting protein that after thrombin-mediated conversion into fibrin forms an insoluble fibrin clot which prevents the loss of blood upon vascular injuries. The fibrin clot also serves as a provisional matrix that participates in subsequent wound healing and other processes through the interaction with various plasma proteins and cell types. Fibronectin is a multifunctional adhesive protein that interacts with a number of macromolecules and surface receptors on a variety of cells, including fibroblasts, neurons, phagocytes, and bacteria. It is well-established that fibronectin can be covalently incorporated into the fibrin clot through the transglutaminase action of factor XIIIa (*1*−*3*). This incorporation appears to affect the adhesion to and migration of cells at sites of fibrin deposition thereby contributing to wound healing and other cell-dependent processes (*4*−*7*).

Both fibrinogen and fibronectin are complex multidomain proteins. The fibronectin molecule consists of two subunits linked together by two disulfide bonds (Figure 1A). Each subunit is formed by a single polypeptide chain; the only difference between the chains in plasma fibronectin is the presence in one of them of a variable region due to alternative splicing. Each chain consists of a number of homologous modules of three types, type I ("finger" modules), type II, and type III, which, in fact, represent independently folded domains (*8*, *9*). These domains are grouped into a number of functional regions: fibrin-binding (Fib-1 and Fib-2), collagen-binding, cell-binding, and heparin-binding. The fibrinogen molecule is more complex (Figure 1B). It consists of two identical disulfide-linked subunits, each of which is formed by three nonidentical polypeptide chains, Aα, Bβ, and γ (*10*, *11*). These chains assemble to form a number of independently folded domains grouped into five structural regions, the central E region, two identical terminal D regions, and two αC regions formed by the COOH-terminal portion of the Aα chains (*12*−*15*). The D-E-D regions account for three nodules, central E and two terminal D, observed by electron microscopy; a fourth nodule observed in some molecules near the central nodule corresponds to interacting αC regions, often being referred to as αC-domains (*16*). X-ray analysis of fibrinogen crystals (*14*) revealed that each terminal nodule actually consists of two elongated structures connected to the central nodule by a triple helical coiled coil connector made up of all three chains. Although the three-dimensional structure of the αC regions is not established yet, numerous studies suggest that each αC region

† This work was supported by National Institutes of Health Grant HL-56051 to L.M.

* To whom correspondence should be addressed at the University of Maryland School of Medicine, Center for Vascular and Inflammatory Diseases, 800 West Baltimore Street, Baltimore, MD 21201. E-mail: Lmedved@som.umaryland.edu. Phone: (410) 706-8065. Fax: (410) 706-8121.

‡ University of Maryland School of Medicine.

§ The George Washington University School of Medicine and Health Sciences.

10.1021/bi7001373 CCC: $37.00
Published on Web 04/11/2007

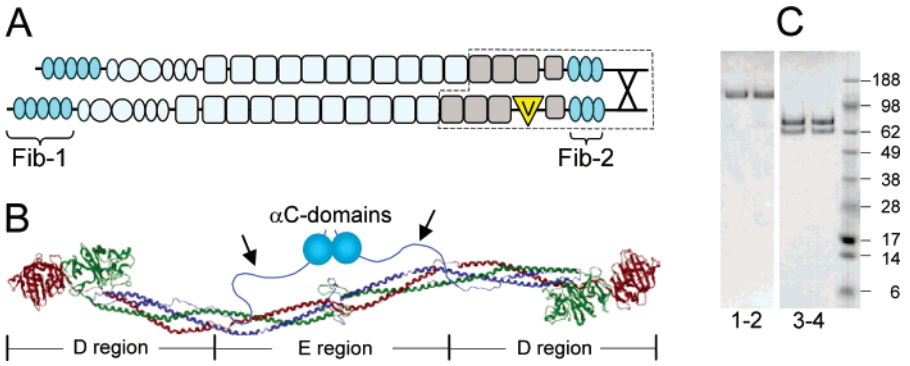

FIGURE 1: Location of the complementary binding sites in fibronectin and fibrin(ogen). Panel A, schematic representation of the fibronectin molecule consisting of two disulfide-linked subunits each of which is composed of type I (ovals), type II (circles), and type III (rectangles) domains; the variable domain in one of the subunits is denoted by "v". The type I "finger" domains involved in formation of the Fib-1 and Fib-2 fibrin binding regions are shown in blue. The region corresponding to the 140 kDa $(Fib\text{-}2)_2$ fragment is highlighted by a broken line. Panel B, ribbon diagram of fibrinogen based upon its crystal structure (*14*). The individual fibrinogen chains, Aα, Bβ and γ, are colored blue, green, and red, respectively; the αC-domains are shown as two spheres attached to the bulk of the molecule with the flexible αC-connectors marked by arrows; the vertical lines denote approximate boundaries between the fibrinogen D and E regions. Panel C, SDS−polyacrylamide gel electrophoresis analysis of the 140 kDa $(Fib\text{-}2)_2$ fragment in nonreduced (lanes 1 and 2) and reduced (lanes 3 and 4) conditions; the right outer lane contains protein markers of the indicated molecular masses (SeeBlue Plus2 Prestained Standards, Invitrogen).

consists of a compact αC-domain attached to the bulk of the molecule with a flexible αC-connector (*12*, *13*, *16*−*18*).

Incorporation of fibronectin into a fibrin clot occurs by noncovalent interaction between the two proteins through specific binding sites, followed by their covalent cross-linking with factor XIIIa. Each fibronectin subunit contains two fibrin-binding regions, Fib-1 and Fib-2, located in its NH_2- and COOH-terminal portions, respectively (*19*, *20*) (Figure 1A). The NH_2-terminal Fib-1 region consists of the first five type I (finger) domains, F1-F2-F3-F4-F5, while the COOH-terminal Fib-2 region includes three such fingers, F10-F11-F12. The noncovalent interaction of the Fib-1 region with fibrin occurs through a pair of the Fib-1 fingers, F4-F5 (*21*−*23*), and the fibrin αC regions (*24*, *25*). The Fib-1 binding site was further localized within the Aα221−391 portion of the αC region (*3*) corresponding to its αC-connector (*17*). This interaction occurs with a relatively high affinity (*3*, *26*), and is proposed to play a role in bringing fibronectin to fibrin and providing proper orientation of the cross-linking sites to facilitate the covalent stage of the interaction (*3*).

Less is known about the interaction of fibronectin with fibrin through the Fib-2 region. Although binding experiments established that fibronectin and its Fib-1 fragment interact with fibrin through the αC regions of the latter (*3*), there is no direct evidence for the involvement of Fib-2 in this interaction. The data about the affinity of Fib-2 to fibrin are also controversial. Our previous study (*21*) revealed that the proteolytically isolated Fib-1 and Fib-2 fragments both bound to fibrin-Sepharose and that Fib-2 was eluted at higher concentration of the urea/NaCl eluting buffer suggesting that its affinity to fibrin should be comparable to or even higher than that of Fib-1. In contrast, Rostagno et al. (*26*) reported that in ELISA[1] experiments the Fib-2 fragment bound to immobilized fibrin with much lower affinity than Fib-1. Based on this finding they hypothesized that the NH_2-terminal site due to its higher affinity may provide primary binding to fibrin, while the COOH-terminal site may serve to subsequently strengthen the interaction (*26*). As an alternative they proposed that the COOH-terminal fibrin-binding site may be an artifact of enzymatic digestion and may not have physiological function (*26*). Thus, while the interaction of fibronectin with fibrin through the Fib-1 region is well characterized and its role in the incorporation of fibronectin into the fibrin clot is established, its interaction through Fib-2 is still poorly understood and the role of this interaction is not clear.

In this study, we prepared two Fib-2 containing fragments, monomeric 19 kDa Fib-2 and dimeric 140 kDa $(Fib\text{-}2)_2$, and characterized their interaction with the recombinant fibrinogen αC region fragment and its subfragments. Direct measurements established that Fib-2 containing fragments interact with the αC region. The Fib-2 binding site was further localized to the NH_2-terminal half of this region, the αC-connector. Experiments also confirmed that Fib-2 has lower affinity to the αC region fragment than Fib-1, and revealed that Fib-1 and Fib-2 bind mainly to different sites, and that some of these sites may overlap. Based on these and the previous results (*3*, *21*, *23*, *26*) we propose a mechanism of interaction of fibronectin with fibrin suggesting a role for both Fib-1 and Fib-2.

EXPERIMENTAL PROCEDURES

Fibronectin and Its Fragments. Fibronectin was purified from human plasma by affinity chromatography on gelatin-Sepharose as described earlier (*27*). NH_2-terminal 29 kDa fibrin-binding fragment, Fib-1, and COOH-terminal 19 kDa fibrin-binding fragment, Fib-2, were prepared from thermolysin digests of fibronectin as described (*21*, *28*). COOH-terminal 140 kDa $(Fib\text{-}2)_2$ fragment, representing a dimeric disulfide-linked COOH-terminal portion of fibronectin which include two Fib-2 regions (Figure 1A), was isolated from the limited cathepsin D digest of fibronectin by affinity chromatography on heparin-Sepharose, as described in ref *29*. The dimeric structure of 140 kDa $(Fib\text{-}2)_2$ was confirmed by SDS−polyacrylamide gel electrophoresis analysis in

[1] Abbreviations: ELISA, enzyme-link immunosorbent assay; SPR, surface plasmon resonance; TBS, tris buffer saline (20 mM tris buffer, pH 7.4, 150 mM NaCl); HBS, HEPES buffer containing 20 mM HEPES, pH 7.4, 150 mM NaCl, 2 mM $CaCl_2$.

reduced conditions, which revealed two chains with apparent molecular masses of 65 and 75 kDa (Figure 1C). In addition, NH_2-terminal sequence analysis of this fragment performed with a Hewelett-Packard G1000A sequencer revealed two sequences starting at Val^{1609} and Ala^{1614}, which are located at the end of 11th type III module.

Recombinant αC-Fragments and αC Oligomers. The recombinant Aα221−610 fragment, corresponding to the human fibrinogen αC region, and its subfragments, Aα221−391 and Aα392−610, corresponding to the αC-connector and αC-domain, respectively, were produced in *Escherichia coli* using the pET-20b expression vector as described earlier (*30*). Soluble cross-linked oligomeric form of the Aα221−610 fragment (αC oligomers), mimicking the structure and properties of the αC regions in cross-linked fibrin, was prepared as described in ref *31*.

Enzymes and Antibodies. Proteolytic enzymes thermolysin (protease type X) and cathepsin D, rabbit anti-fibronectin polyclonal antibodies, and anti-rabbit IgG-horseradish conjugate were purchased from Sigma-Aldrich. Anti-Fib-2 polyclonal antibodies were prepared by affinity chromatography of anti-fibronectin polyclonal antibodies on 19 kDa Fib-2 fragment-Sepharose.

Solid-Phase Binding Assay. Solid-phase binding was performed in plastic microtiter plates using an enzyme-link immunosorbent assay, ELISA. Microtiter plate wells (Fisher) were coated overnight with 100 μL/well of 20 μg/mL Aα221−610 αC-fragment or its subfragments, Aα221−391 and Aα392−610, in 100 mM $NaHCO_3$, pH 8.3. The wells were blocked with Casein Blocker (Pierce) for 1 h at 37 °C. Following washing with TBS-Tween-20 (20 mM Tris buffer, pH 7.4, containing 150 mM NaCl and 0.05% Tween-20), the indicated concentrations of the fibronectin Fib-2 or 140 kDa $(Fib\text{-}2)_2$ fragments were added to the wells and incubated for 2 h at 4 °C. The bound fibronectin fragments were detected by reaction with rabbit anti-fibronectin polyclonal antibodies, followed by peroxidase-conjugated anti-rabbit IgG. A TMB Microwell Peroxidase Substrate (Kirkengaard & Perry Laboratories Inc.) was added to the wells, and the amount of bound ligand was measured spectrophotometrically at 450 nm. Data were analyzed by nonlinear regression analysis using eq 1,

$$A = A_{max}/(1 + K_d/[L]) \quad (1)$$

where A represents absorbance of the oxidized substrate, which is assumed to be proportional to the amount of ligand bound, A_{max} is the concentration of ligand bound at saturation, [L] is the molar concentration of free ligand, and K_d is the dissociation constant.

Ligand Blotting Assay. The αC-fragment and subfragments were subjected to SDS−polyacrylamide gel electrophoresis using NuPAGE BisTris electrophoretic system (Invitrogen) and then electrotransferred to a nitrocellulose membrane. To check if the transfer was successful, the membrane was stained with 0.5% Ponseau S for 1 min followed by washing with deionized water and destaining with 5% acetic acid. The membrane was blocked for 1 h with Casein Blocker (Pierce), followed by incubation with 20 μg/mL 140 kDa $(Fib\text{-}2)_2$ for 2 h at 4 °C. The bound 140 kDa $(Fib\text{-}2)_2$ fragment was detected by reaction with rabbit anti-fibronectin polyclonal antibodies and peroxidase-conjugated anti-rabbit IgG. Visualization of the peroxidase-labeled protein bands was performed by the procedure recommended by the manufacturer using SuperSignal West Pico Chemiluminescent Substrate (Pierce).

Surface Plasmon Resonance Analysis. The interaction of fibronectin and its fragments with the recombinant Aα220−610 αC-fragment was studied by surface plasmon resonance (SPR) using the IAsys biosensor (Fisons, Cambridge, U.K.). The Aα220−610 fragment was covalently coupled to the activated carboxymethyldextran-coated sensor surface by the procedure recommended by the manufacturer. Binding experiments were performed in TBS containing 0.05% Tween 20, 0.02% NaN_3, and 0.1 mM PMSF (TBS binding buffer) at room temperature. The association between the immobilized αC-fragment and the added fibronectin or its fragments was monitored as a change in the SPR response. To regenerate the surface, complete dissociation of the complex was achieved by adding 3 M guanidinium chloride for 0.5 min, followed by re-equilibration with TBS binding buffer. The data were analyzed using the FASTfit program supplied with the instrument. This program uses an iterative curve-fitting to derive the observed rate constant (termed on-rate constant in FASTfit), and the maximum response at equilibrium due to ligand binding at the particular ligand concentration (termed Extent in FASTfit). The analysis was performed as previously described in detail (*32*). Briefly, the association curves at each concentration of ligand were fitted to a pseudo-first-order equation to derive the observed rate constant (k_{obs}). Then the concentration dependence of k_{obs} was fitted to eq 2,

$$k_{obs} = k_{diss} + k_{ass}[\text{ligand}] \quad (2)$$

to derive the association rate constant (k_{ass}) from the slope and the dissociation rate constant (k_{diss}) from the intercept. The equilibrium dissociation constant (K_d) was calculated as $K_d = k_{diss}/k_{ass}$. Alternatively, the association curves were used to derive the maximal response at the equilibrium for each fibronectin concentration (Extent), which is actually proportional to the bound fibronectin. The binding data (Extent versus concentration plot) were used to construct Scatchard plots and to determine the equilibrium dissociation constants.

SPR experiments on interaction of fibronectin with the oligomeric form of the Aα221−610 fragment were performed using the BIAcore 3000 biosensor (BIAcore AB, Uppsala, Sweden). This form was covalently coupled to the activated surface of a CM5 sensor chip using the amine coupling kit (BIAcore AB), as specified by the manufacturer. Binding experiments were performed in HBS buffer containing 20 mM HEPES, pH 7.4, 2 mM $CaCl_2$, 150 mM NaCl, 0.005% Tween 20 (HBS binding buffer) at a flow rate of 20 μL/min and room temperature. Samples at different concentrations were injected in duplicate, and the association between the immobilized Aα220−610 fragment and the added fibronectin was monitored as the change in the SPR response. To regenerate the chip surface, complete dissociation of the complex was achieved by adding 3 M guanidinium chloride for 30 s followed by re-equilibration with HBS binding buffer. Experimental data were analyzed as described above using BIAevaluation 3.1 software supplied with the instrument.

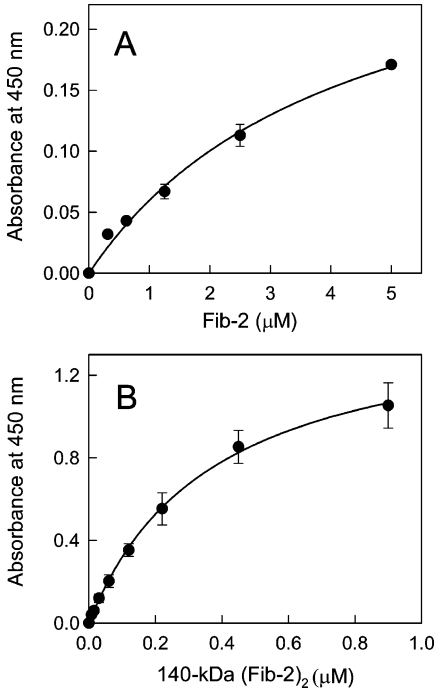

FIGURE 2: Analysis of binding of the fibronectin fibrin-binding fragments to the Aα221−610 fragment by ELISA. Increasing concentrations of the Fib-2 (panel A) or 140 kDa (Fib-2)$_2$ (panel B) fragments were incubated with the microtiter wells coated with the Aα221−610 fragment, and the bound fragments were detected with anti-fibronectin polyclonal antibodies. The curves for each fragment represent the best fit of the date to eq 1. Errors bars reflect the standard deviation of duplicate experiments.

Table 1: Dissociation Constants (K_d) for the Interaction of the Fibrin-Binding Fragments of Fibronectin with the Recombinant Aα221−610 αC-Fragment and Its Subfragments[a]

αC-fragments	K_d, nM Fib-1	K_d, μM 19 kDa Fib-2	K_d, nM 140 kDa (Fib-2)$_2$
Aα221−610	36[b]	3.1 ± 0.4[c]	360 ± 70[c]
		2.5 ± 0.3[d]	410 ± 60[d]
Aα221−391			760 ± 80[c]
Aα392−610			no binding[c]

[a] Values are means ± the standard deviation of at least three independent experiments. [b] Obtained by SPR in the previous study (*3*). [c] Obtained by ELISA. [d] Obtained by SPR.

RESULTS

Interaction between the Recombinant αC Region of Fibrin-(ogen) and the Fib-2-Containing Fragments of Fibronectin. It is well-established that fibrin interacts with fibronectin through the NH_2-terminal Fib-1 and COOH-terminal Fib-2 regions of the latter. Our previous study (*3*) revealed that this interaction occurs through the fibrin αC regions and localized the Fib-1 binding sites to the αC-connector portions of these regions. In this study we focused on the interaction mediated by the Fib-2 regions. First, we tested in direct experiments whether the isolated Fib-2 fragment interacts with the recombinant αC region. In ELISA, the proteolytically prepared monomeric 19 kDa Fib-2 fragment bound to the immobilized recombinant Aα221−610 fragment, which corresponds to the αC region, in a dose-dependent manner (Figure 2A). However, the affinity of this interaction (K_d = 3.1 μM) was low (Table 1). Since proteolysis may influence the properties of the Fib-2 region and since there are two such regions in the parent molecule, we next prepared and studied a dimeric 140 kDa (Fib-2)$_2$ fragment corresponding to the COOH-terminal portion of fibronectin with two Fib-2 regions (Figure 1A). This fragment bound to the immobilized Aα221−610 fragment with higher affinity (K_d = 360 nM). To further evaluate the affinities of these interactions, we used another method, surface plasmon resonance (SPR). When the Aα221−610 fragment was immobilized to the surface of a sensor chip, it bound both the Fib-2 monomer and the 140 kDa (Fib-2)$_2$ dimer in a dose-dependent manner (Figure 3). The K_d values calculated using the observed rate constants, as described in Experimental Procedures, were found to be 2.5 μM and 410 nM for the monomer and dimer, respectively (Table 1). They are similar to those determined by ELISA. These results indicate that the Fib-2 regions of fibronectin interact with the fibrin(ogen) αC regions, and that their affinity to this region is lower than that of Fib-1. Since the Fib-2 region seems to be better preserved in 140 kDa (Fib-2)$_2$, all further experiments have been performed with this fragment.

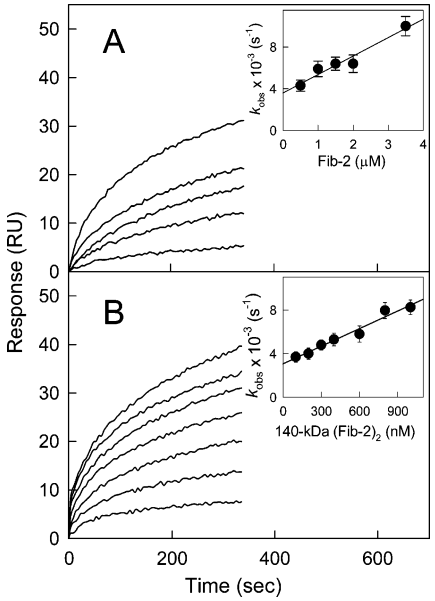

FIGURE 3: Analysis of binding of the fibronectin fibrin-binding fragments to the Aα221−610 fragment by surface plasmon resonance. Increasing concentrations of the Fib-2 (panel A) or 140 kDa (Fib-2)$_2$ (panel B) fragments were added to the immobilized Aα221−610 fragment, and their association was monitored in real time while registering the resonance signal (response) by IAsys biosensor. The concentrations in panel A were 0.5, 1.0, 1.5, 2.0, and 3.5 μM, and those in panel B were 50, 100, 200, 300, 400, 600, and 800 nM, respectively. The inset in each panel shows a plot of the values of k_{obs} determined for each association curve versus ligand concentration to derive k_{ass} and k_{diss} and thus determine the dissociation equilibrium constant, K_d.

Localization of the Fib-2 Binding Sites in the Fibrin(ogen) αC-Connector. To further localize the Fib-2 binding sites within the fibrin(ogen) αC region, we first used ligand blotting assay. The recombinant Aα221−610 fragment and its subfragments, Aα221−391 and Aα392−610, corresponding to the αC-connector and αC-domain, respectively (*17*), were electrophoresed in 10% polyacrylamide gel, transferred onto nitrocellulose membrane, and then probed with the 140 kDa (Fib-2)$_2$ fragment. The experiment revealed that 140 kDa (Fib-2)$_2$ bound to the Aα221−610 fragment and its Aα221−391 subfragment, while no binding was observed with the other subfragment, Aα392−610 (Figure 4). This

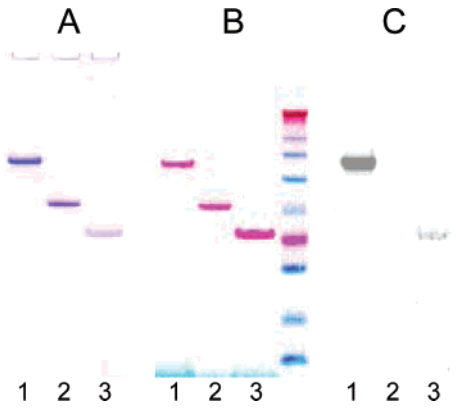

FIGURE 4: Analysis of binding of the 140 kDa (Fib-2)$_2$ fragment to the Aα221−610 αC-fragment and its subfragments by ligand blotting. The Aα221−610 fragment and its subfragments, Aα392−610 and Aα221−391 (lines 1, 2, and 3, respectively), were electrophoresed in 10% polyacrylamide gels that were subsequently stained with Coomassie Blue (panel A) or electrophoretically transferred to nitrocellulose membrane, stained with Ponseau S (panel B), and probed with the 140 kDa (Fib-2)$_2$ fragment after destaining (panel C). Bound 140 kDa (Fib-2)$_2$ in panel C was detected as described in Experimental Procedures. The right outer lane in panel B contains molecular mass markers.

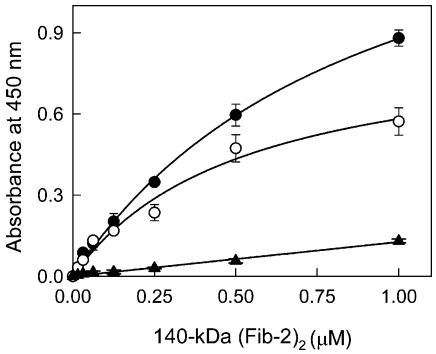

FIGURE 5: Analysis of binding of the 140 kDa (Fib-2)$_2$ fragment to the Aα221−610 αC-fragment and its subfragments by ELISA. Increasing concentrations of 140 kDa (Fib-2)$_2$ were incubated with microtiter wells coated with the αA221−610 fragment (open circle), or its subfragments, Aα221−391 (solid circle) and Aα392−610 (triangles), and bound 140 kDa (Fib-2)$_2$ was detected with anti-fibronectin polyclonal antibodies. The curves for the Aα221−610 and Aα221−391 fragments represent the best fit of the date to eq 1. Error bars reflect the standard deviation of the duplicate experiments.

suggests that the Fib-2 binding site is located within the Aα221−391 residues forming the αC-connector. However, binding of 140 kDa (Fib-2)$_2$ to the Aα221−391 subfragment seems to be relatively weak since the intensity of the band corresponding to this subfragment was quite low (Figure 4C). To further confirm this binding we tested the interaction between these components by ELISA. When 140 kDa (Fib-2)$_2$ at increasing concentrations was incubated with immobilized Aα221−610 and its subfragments, it exhibited a dose-dependent binding to Aα221−610 and Aα221−391, while no binding to the Aα392−610 subfragment was observed (Figure 5). In contrast to the results of ligand blotting, in this assay the binding of 140 kDa (Fib-2)$_2$ to the Aα221−391 fragment (K_d = 760 nM) was comparable with its binding to the Aα221−610 subfragment (K_d = 360 nM) (Table 1). Altogether these results indicate that the Fib-2 binding site is located in the fibrin(ogen) αC-connector including residues Aα221−391.

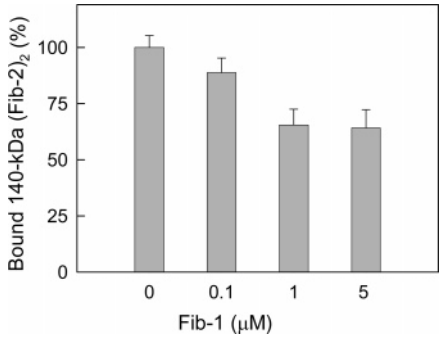

FIGURE 6: Competition experiment on the binding of the Fib-1 and 140 kDa (Fib-2)$_2$ fragments to the immobilized Aα221−610 αC fragment performed by ELISA. The 140 kDa (Fib-2)$_2$ fragment at 0.25 μM in the presence of increasing concentrations of the Fib-1 fragment was incubated with microtiter wells coated with 20 μg/mL Aα221−610. Bound 140 kDa (Fib-2)$_2$ was detected with anti-Fib-2 polyclonal antibodies. Error bars reflect the standard deviation of three independent experiments.

Competition Experiments. This and the previous study (*3*) localized the Fib-1 and Fib-2 binding sites within the fibrin(ogen) αC-connector. Since both the Fib-1 and Fib-2 regions consist of homologous repeats, type I (finger) domains, and bind to the same αC-connector, one might expect that they share the same binding site(s). Alternatively, Fib-1 and Fib-2 may bind to different sites. To select between these alternatives, we performed the following competition experiments. In ELISA, when 140 kDa (Fib-2)$_2$ at 0.25 μM was incubated with the immobilized Aα221−610 fragment in the presence of increasing concentrations of the Fib-1 fragment, the latter inhibited binding of the former only moderately (Figure 6). Even at the concentration of 5 μM, which is more than 100-fold higher than the K_d value for the interaction of Fib-1 with the αC-fragment, the Fib-1 fragment inhibited the binding by only about 30%. These results are in agreement with the previous observation (*23*), in which the recombinant F4-F5 fragment of the fibronectin Fib-1 region and the anti-F4-F5 monoclonal antibody only partially inhibited binding of fibronectin to immobilized fibrin. They also suggest that the fibrin(ogen) αC-connector contains more than one fibronectin binding site, and that the Fib-1 and Fib-2 regions of fibronectin interact with the αC-connector mainly through different sites, but that some of these sites may overlap.

SPR-Detected Interaction of Fibronectin with the Aα221−610 Fragment. The experiments with the isolated Fib-1 and Fib-2 containing fragments performed here and before (*3*, *23*, *26*) suggest that there should be at least two types of fibrin-binding sites in fibronectin, one of high affinity and another one of lower affinity. At the same time, in the previous studies (*3*, *23*, *26*) only the high affinity binding of fibronectin to either immobilized fibrin or its recombinant αC-fragments has been observed. To check if a lower affinity binding between these proteins could also be detected, we studied the interaction between fibronectin and the immobilized Aα221−610 fragment by SPR using a wide range of fibronectin concentrations (Figure 7). When fibronectin was added at low concentrations (2.5−25 nM), it exhibited a dose-dependent interaction with Aα221−610. The K_d value calculated using the observed rate constants, k_{obs} (see Experimental Procedures), was found to be 13 nM (inset A and Table 2). This value is comparable with that determined earlier for the interaction between these species by the same

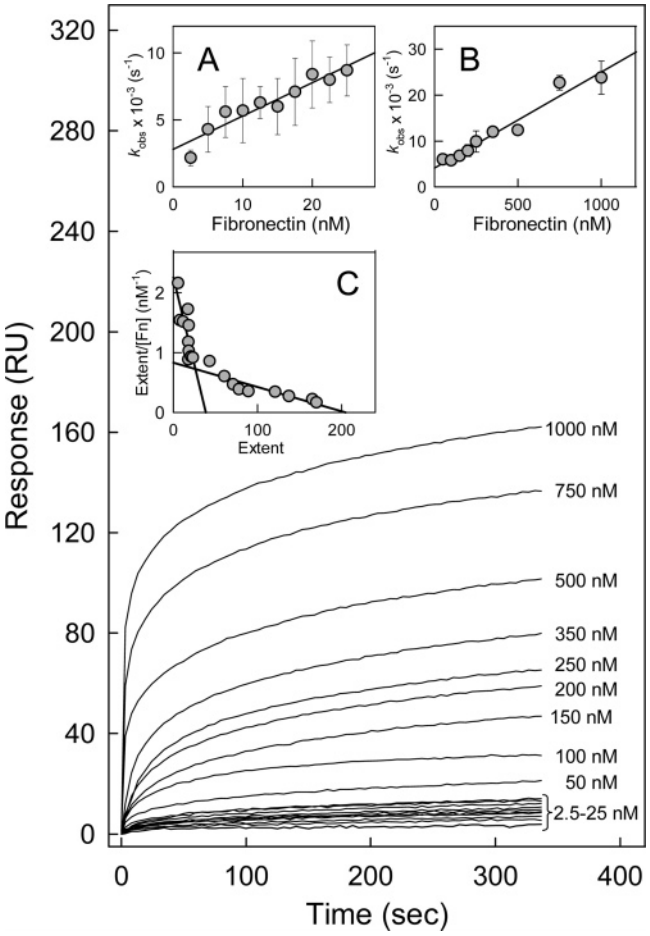

FIGURE 7: Binding of fibronectin to the Aα221−610 αC-fragment detected by surface plasmon resonance. Fibronectin at the indicated concentrations (2.5−25 nM includes 2.5, 5, 7.5, 10, 12.5, 15, 17.5, 20, 22.5, and 25 nM) was added to the immobilized Aα221−610 fragment, and its association was monitored in real time while registering the resonance signal (response) using the IAsys biosensor. Insets A and B show plots of the k_{obs} values determined for each association curve in the 2.5−25 nM and 50−1000 nM concentration ranges, respectively, versus ligand concentration to derive k_{ass} and k_{diss} and thus determine the dissociation equilibrium constants (K_d) presented in Table 2. Error bars in both insets reflect the standard deviation of four independent experiments. Inset C shows an alternative analysis of the association data obtained in the 2.5−1000 nM concentration range. The maximum responses at equilibrium (Extent) expressed in response units (RU) were plotted versus fibronectin concentration ([Fn]) to obtain the saturable binding curve and to construct the Scatchard plot shown in the inset and determine the equilibrium dissociation constants presented in Table 2.

method (*3*) (Table 1). When fibronectin was added at higher concentrations (50−1000 nM), a substantial increase in binding was observed, suggesting the presence of a lower affinity binding site(s). The K_d value calculated from the analysis of the binding curves obtained in this concentration range was found to be 220 nM (inset B and Table 2). This value is close to those calculated for the interaction of the 140 kDa $(Fib\text{-}2)_2$ fragment with immobilized Aα221−610 (Table 1). The presence in the αC region of two classes of fibronectin-binding sites with different affinities is more graphically illustrated by an alternative analysis of the association curves presented in Figure 7. The curves were employed to derive the maximal response at equilibrium (Extent) for each fibronectin concentration, which is actually proportional to the bound fibronectin. These data were used

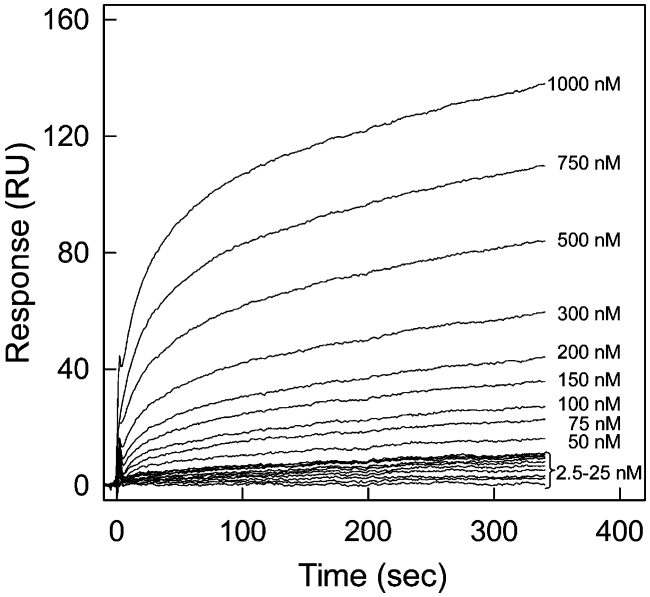

FIGURE 8: Binding of fibronectin to αC oligomers detected by surface plasmon resonance. Fibronectin at the indicated concentrations (2.5−25 nM includes 2.5, 5, 7.5, 10, 12.5, 15, 17.5, 20, 22.5, and 25 nM) was added to the immobilized oligomeric form of the Aα221−610 fragment, and its association was monitored in real time while registering the resonance signal (response) using the BIAcore 3000 biosensor. The data were analyzed as described in the text to obtain the K_d values shown in Table 2.

Table 2: Dissociation Constants (K_d) for the Interaction of Fibronectin with the Recombinant Aα221−610 αC-Fragment and Its Cross-Linked αC Oligomers Obtained by Analyses of the SPR Data[a]

fragment	K_{d1}, nM	K_{d2}, nM
αC monomer	13 ± 3[b]	220 ± 21[c]
	16[d]	250[d]
αC oligomer	11 ± 2.5[b]	670 ± 85[c]
	15[d]	550[d]

[a] Values are means ± the standard deviation of 2−4 independent experiments. [b] Obtained by the analysis of association data in the 2.5−25 nM concentration range. [c] Obtained by the analysis of association data in the 50−1000 nM concentration range. [d] Obtained by the Scatchard analysis.

to construct a Scatchard plot, which revealed two types of binding sites with the K_d values of 16 and 250 nM (inset C and Table 2). The relative number of weak versus strong sites was approximately 4:1. These data clearly indicate that fibronectin interacts with the fibrin(ogen) αC regions through two types of binding sites, high affinity and low affinity, with a greater number of the latter.

Since fibronectin interacts only with fibrin (*3*), and since in fibrin the αC regions form αC polymers (*16*), we next studied binding of fibronectin to the immobilized cross-linked oligomeric form of the Aα221−610 fragment (αC oligomers), which mimics such polymers (*31*, *33*). The SPR experiments performed in the same concentration range of fibronectin as above (2.5−1000 nM) revealed that the character of association of this protein with immobilized αC oligomers (Figure 8) was similar to that of fibronectin with the Aα221−610 monomer presented in Figure 7. The K_d values calculated as described above using the observed rate constants determined in the 2.5−25 nM and 50−1000 nM concentration ranges were found to be 11 and 670 nM, respectively (Table 2). The Scatchard plot (not shown) was

similar to that in Figure 7, inset C, with K_d values of 15 and 550 nM. These results further confirm that the interaction of fibronectin with the αC regions occurs through two types of binding sites, high affinity and low affinity. They also suggest that the affinities of these sites do not change substantially upon polymerization of these regions in fibrin.

DISCUSSION

Noncovalent binding of fibronectin to fibrin plays an important role in the covalent incorporation of the former into the fibrin clot. Previous studies identified two fibrin-binding regions in fibronectin, Fib-1 and Fib-2 (*19*, *20*), and established the mechanism of the Fib-1 mediated interaction (*3*, *21*, *23*). The major goal of the present study was to characterize the interaction mediated by the Fib-2 region and clarify its role in the incorporation of fibronectin into the clot. The Fib-1 and Fib-2 fragments corresponding to the fibrin-binding regions can be prepared by limited proteolysis of fibronectin with various enzymes. Comparison of the fibrin-binding properties of these fragments performed previously by two groups (*21*, *26*) gave quite conflicting results. While ELISA revealed that Fib-2 bound to immobilized fibrin with a much lower affinity than Fib-1 (*26*), the results of affinity chromatography experiments suggested that their affinities may be comparable (*21*, *26*). Such a discrepancy may arise from several factors. First, the use of affinity chromatography for comparison of relative affinities of proteins may have some limitations, as discussed in ref *26*. Second, although ELISA is widely used for determination of equilibrium dissociation constants, their absolute values are often dependent on experimental conditions (*3*, *34*, *35*). Finally, the 14.4 kDa Fib-2 fragment used in the ELISA experiments described in ref *26* was prepared from a subtilisin digest of fibronectin and contained proteolytic cleavages in the F12 domain, which was shown to be important for fibrin-binding. To minimize these factors, we used the 19 kDa Fib-2 and 140 kDa $(Fib\text{-}2)_2$ fragments prepared from the thermolysin and cathepsin D digests of fibronectin, respectively, which were devoid of the above-mentioned cleavages; we also used a real-time binding assay, SPR, in addition to a solid-phase binding assay, ELISA.

The present study confirmed our previous prediction (*3*) that the Fib-2 region of fibronectin should interact with the αC region of fibrin. The study also revealed that affinities of Fib-2 containing fragments to the αC region depend on their composition. Of the two tested Fib-2 containing fragments, 140 kDa $(Fib\text{-}2)_2$ and 19 kDa Fib-2, the former, which being bivalent better mimics the Fib-2 regions of the parent protein, had a higher affinity. At the same time, its binding was still more than 10-fold weaker than that of the Fib-1 fragment (Table 1). In agreement, SPR experiments with whole fibronectin revealed two classes of binding sites with dissociation constants comparable to those determined for the Fib-1 and the 140 kDa $(Fib\text{-}2)_2$ fragments (Tables 1 and 2). It should be noted that a similar difference between the ELISA-determined dissociation constants for the interaction of Fib-1 and Fib-2 with fibrin was reported in ref *26*. Altogether, these results clearly indicate that affinity of the Fib-2 region to the αC region is about 1 order of magnitude lower than that of Fib-1.

Our binding experiments revealed that the amount of fibronectin bound to immobilized αC through the low affinity sites (Fib-2 binding) is higher than that through the high affinity ones (Fib-1 binding). This implies that each αC region contains several fibronectin binding sites and that there are more sites for Fib-2 than for Fib-1. Although the data did not allow calculating the absolute number of each type of binding site, the Scatchard analysis suggests that the number of Fib-2 sites exceeds that of Fib-1 by approximately 4-fold. Thus, if each αC region contains one high affinity Fib-1 site, it should have at least four additional low affinity Fib-2 sites. Further, the competition experiments revealed that at least one of the Fib-2 sites of the αC region overlaps with the Fib-1 site. This implies that the interaction of fibronectin through Fib-1 is more specific than through Fib-2.

Previously, Rostagno et al. (*21*) hypothesized that the Fib-1 sites, due to their higher affinity, may provide primary binding to fibrin, while the Fib-2 sites may serve to subsequently strengthen the interaction. Since the primary interaction is reinforced by covalent cross-linking of Fib-1 to the αC region, the strengthening role of the Fib-2 mediated interaction might seem superfluous. In this case one can propose an alternative hypothesis. Namely, since fibronectin is a long multidomain flexible molecule and Fib-1 binding anchors to fibrin only its NH_2-terminal portions, Fib-2 binding may serve to additionally anchor the COOH-terminal portions thereby immobilizing the entire molecule in a particular conformation on the fibrin surface. It should be noted that the αC regions in fibrin are located in close proximity forming covalently cross-linked αC polymers (*16*) and that the length of the fibronectin molecule substantially exceeds that of an individual αC region. This implies that the Fib-1 and Fib-2 regions of the same fibronectin molecule could be anchored to the αC regions of different fibrin molecules.

In the present study, we found that the Fib-2 binding site, like that of Fib-1 (*3*), is located within the αC-connector portion of the αC region. This portion contains ten 13-residue internal tandem repeats (*36*) and has a flexible extended conformation (*16*, *17*). Previous studies also established that at least two adjacent finger domains are involved in the binding of Fib-1 and Fib-2 to fibrin (*21*, *23*, *26*). These findings indicate that the interaction of both Fib-1 and Fib-2 regions of fibronectin with the αC-connector occurs through a combination of adjacent finger domains in each of the former and flexible tandem repeats of the latter. This is reminiscent of the interaction of the Fib-1 region with some bacterial fibronectin-binding proteins (FnBPs) (*37*−*41*). Recent NMR studies established that this interaction occurs through a "tandem β-zipper" mechanism whereby the unstructured regions of the tandem repeats in FnBP form additional antiparallel β-strands at the edges of the triple-stranded β-sheets of adjacent finger domains of fibronectin (*38*, *39*). It is interesting that the length of two extended αC-connector repeats is similar to the length of the streptococcal FnBP peptide B3 that associates with the bimodular fibronectin fragment F1-F2 in the complex solved by NMR (*38*). It is also comparable with the length of a staphylococcal FnBP peptide that interacts with another bimodular fibronectin fragment, F4-F5 (*42*). Further, our molecular modeling revealed that a pair of the αC-connector repeats can be accommodated on the FnBP-binding surface of the F4-F5 fragment (results not shown). All these facts suggest that

the interaction of fibronectin with fibrin could also occur through a "tandem β-zipper" mechanism.

In summary, based on this and the previous studies (*3*, *21*, *23*, *26*) one can suggest the following mechanism of incorporation of fibronectin into fibrin clots. The primary high affinity noncovalent interaction between fibronectin and fibrin occurs through the NH_2-terminal Fib-1 region (F4-F5 domains) of the former and the αC-connectors (tandem repeats) of the latter. This interaction is highly specific and should be sufficient to facilitate covalent cross-linking by factor XIIIa, which further reinforces the complex. The Fib-1 mediated binding also increases the local concentration of fibronectin thereby facilitating its Fib-2 mediated lower affinity interaction with fibrin. This interaction is less specific, may occur through any of several low affinity sites, and serves most probably to anchor the COOH-terminal portions of the fibronectin molecule to the fibrin clot. Such anchoring may play an important role in immobilizing fibronectin on a fibrin surface in a particular conformation, perhaps exposing cryptic binding sites (*43*−*45*) and facilitating its interaction with various molecules and cell types during hemostasis, wound healing, and other processes.

ACKNOWLEDGMENT

We thank Dr. I. Pechik for helpful discussions and criticism.

REFERENCES

1. Mosher, D. F., and Johnson, R. B. (1983) In vitro formation of disulfide-bonded fibronectin multimers, *J. Biol. Chem. 258*, 6595−6601.
2. Matsuka, Y. V., Migliorini, M. M., and Ingham, K. C. (1997) Cross-linking of fibronectin to C-terminal fragments of the fibrinogen α-chain by factor XIIIa, *J. Protein Chem. 16*, 739−745.
3. Makogonenko, E., Tsurupa, G., Ingham, K., and Medved, L. (2002) Interaction of fibrin(ogen) with fibronectin: further characterization and localization of the fibronectin-binding site, *Biochemistry 41*, 7907−7913.
4. Grinnell, F., Feld, M., and Minter, D. (1980) Fibroblast adhesion to fibrinogen and fibrin substrata: requirement for cold-insoluble globulin (plasma fibronectin), *Cell 19*, 517−525.
5. Knox, P., Crooks, S., and Rimmer, C. S. (1986) Role of fibronectin in the migration of fibroblasts into plasma clots, *J. Cell Biol. 102*, 2318−2323.
6. Corbett, S. A., Wilson, C. L., and Schwarzbauer, J. E. (1996) Changes in cell spreading and cytoskeletal organization are induced by adhesion to a fibronectin-fibrin matrix, *Blood 88*, 158−166.
7. Corbett, S. A., Lee, L., Wilson, C. L., and Schwarzbauer, J. E. (1997) Covalent cross-linking of fibronectin to fibrin is required for maximal cell adhesion to a fibronectin-fibrin matrix, *J. Biol. Chem. 272*, 24999−25005.
8. Odermatt, E., Tamkun, J. W., Hynes, R. O. (1985) Repeating modular structure of the fibronectin gene: relationship to protein structure and subunit variation, *Proc. Natl. Acad. Sci. U.S.A. 82*, 6571−6575.
9. Tatunashvili, L. V., Filimonov, V. V., Privalov, P. L., Metsis, M. L., Koteliansky, V. E., Ingham, K. C., and Medved, L. V. (1990) Co-operative domains in fibronectin, *J. Mol. Biol. 211*, 161−169.
10. Doolittle, R. F. (1984) Fibrinogen and fibrin, *Annu. Rev. Biochem. 53*, 195−229.
11. Henschen, A., and McDonagh, J. (1986) Fibrinogen, fibrin and factor XIII, in *Blood Coagulation* (Zwaal, R.F.A., and Hemker, H.C., Eds.) pp 171−241, Elsevier Science Publishers, Amsterdam.
12. Privalov, P. L., and Medved, L. V. (1982) Domains in the fibrinogen molecule, *J. Mol. Biol. 159*, 665−683.
13. Medved, L. V., Gorkun, O. V., and Privalov, P. L. (1983) Structural organization of C-terminal parts of fibrinogen Aα-chains, *FEBS Lett. 160*, 291−295.
14. Yang, Z., Kollman, J. M., Pandi, L., and Doolittle, R. F. (2001) Crystal structure of native chicken fibrinogen at 27 Å resolution, *Biochemistry 40*, 12515−12523.
15. Madrazo, J., Brown, J. H., Litvinovich, S., Dominguez, R., Yakovlev, S., Medved, L., and Cohen, C. (2001) Crystal structure of the central region of bovine fibrinogen (E_5 fragment) at 1.4-Å resolution, *Proc. Natl. Acad. Sci. U.S.A. 98*, 11967−11972.
16. Weisel, J. W., and Medved, L. (2001) The structure and function of the αC domains of fibrinogen, *Ann. N.Y. Acad. Sci. 936*, 312−327.
17. Tsurupa, G., Tsonev, L., and Medved, L. (2002) Structural organization of the fibrin(ogen) αC-domain, *Biochemistry 41*, 6449−6459.
18. Burton, R. A., Tsurupa, G., Medved, L., and Tjandra, N. (2006) Identification of an ordered compact structure within the recombinant bovine fibrinogen αC-domain fragment by NMR, *Biochemistry 45*, 2257−2266.
19. Seidl, M., and Hormann, H. (1983) Affinity chromatography on immobilized fibrin monomer, IV. Two fibrin-binding peptides of a chymotryptic digest of human plasma fibronectin, *Hoppe-Seyler's Z. Physiol. Chem. 364*, 83−92.
20. Hynes, R. O. (1990) Structure of fibronectins, in *Fibronectins* (Rich, A., Ed.) pp 113−175, Springer-Verlag, New York.
21. Matsuka, Y. V., Medved, L. V., Brew, S. A., and Ingham, K. C. (1994) The NH_2-terminal fibrin-binding site of fibronectin is formed by interacting fourth and fifth finger domains. Studies with recombinant finger fragments expressed in Escherichia coli, *J. Biol. Chem. 269*, 9539−9546.
22. Williams, M. J., Phan, I., Harvey, T. S., Rostagno, A., Gold, L. I., and Campbell, I. D. (1994) Solution structure of a pair of fibronectin type 1 modules with fibrin binding activity, *J. Mol. Biol. 235*, 1302−1311.
23. Rostagno, A., Williams, M. J., Baron, M., Campbell, I. D., and Gold, L. I. (1994) Further characterization of the NH_2-terminal fibrin-binding site on fibronectin, *J. Biol. Chem. 269*, 31938−31945.
24. Stathakis, N. E., and Mosesson, M. W. (1977) Interactions among heparin, cold-insoluble globulin, and fibrinogen in formation of the heparin-precipitable fraction of plasma, *J. Clin. Invest. 60*, 855−865.
25. Kirschbaum, N. E., and Budzynski, A. Z. (1990) A unique proteolytic fragment of human fibrinogen containing the Aα COOH-terminal domain of the native molecule, *J. Biol. Chem. 265*, 13669−13676.
26. Rostagno, A. A., Schwarzbauer, J. E., and Gold, L. I. (1999) Comparison of the fibrin-binding activities in the N- and C-termini of fibronectin, *Biochem. J. 338*, 375−386.
27. Miekka, S. I., Ingham, K. C., and Menache, D. (1982) Rapid methods for isolation of human plasma fibronectin, *Thromb. Res. 27*, 1−14.
28. Borsi, L., Castellani, P., Balza, E., Siri, A., Pellecchia, C., De Scalzi, F., and Zardi, L. (1986) Large-scale procedure for the purification of fibronectin domains, *Anal. Biochem. 155*, 335−345.
29. Richter, H., and Hormann, H. (1983) A large cathepsin D-derived fragment from the central part of the fibronectin subunit chains, *FEBS Lett. 155*, 317−320.
30. Tsurupa, G., and Medved, L. (2001) Identification and characterization of novel tPA- and plasminogen-binding sites within fibrin(ogen) αC-domains, *Biochemistry 40*, 801−808.
31. Tsurupa, G. T., Veklich, Y., Hantgan, R., Belkin, A. M., Weisel, J. W., and Medved, L. (2004) Do the isolated fibrinogen αC-domains form ordered oligomers?, *Biophys. Chem. 11*, 257−266.
32. Gorgani, N. N., Parish, C. R., and Altin, J. G. (1999) Differential binding of histidine-rich glycoprotein (HRG) to human IgG subclasses and IgG molecules containing kappa and lambda light chains, *J. Biol. Chem. 274*, 29633−29640.
33. Belkin, A. M., Tsurupa, G., Veklich, Y., Weisel, J. W., and Medved, L. (2005) Transglutaminase-mediated oligomerization of the fibrin(ogen) αC domains promotes integrin-dependent cell adhesion and signaling, *Blood 105*, 3561−3568.
34. Novokhatny, V., Medved, L., Lijnen, R., and Ingham, K. (1995) Tissue-type plasminogen activator interacts with urokinase-type plasminogen activator via its lysine-binding site: an explanation of the poor fibrin affinity of tPA/uPA chimeric molecule, *J. Biol. Chem. 270*, 8680−8685.
35. Yakovlev, S., Zhang, L., Ugarova, T., and Medved, L. (2005) Interaction of fibrinogen with leukocyte receptor $\alpha_M\beta_2$ (Mac-1):

Further characterization and identification of a novel binding region within the central domain of fibrinogen γ-module, *Biochemistry 44*, 617−626.
36. Doolittle, R. F., Watt, K. W. K., Cottrell, B. A., Strong, D. D., and Riley, M. (1979) The amino acid sequence of the α-chain of human fibrinogen, *Nature 280*, 464−468.
37. Ingham, K. C., Brew, S., Vaz, D., Sauder, D. N., and McGavin, M. J. (2004) Interaction of *Staphylococcus aureus* fibronectin-binding protein with fibronectin, Affinity, stoichiometry, and modular requirements, *J. Biol. Chem. 279*, 42945−42953.
38. Schwarz-Linek, U., Werner, J. M., Picford, A. R., Gurusiddappa, S., Kim, J. H., Pilka, E. S., Briggs, J. A. G., Gough, T. S., Hook, M., Campbell, I. D., and Potts, J. R. (2003) Pathogenic bacteria attach to human fibronectin through a tandem β-zipper, *Nature 423*, 177−181.
39. Schwarz-Linek, U., Hook, M., and Potts, J. R. (2004) The molecular basis of fibronectin-mediated bacterial adherence to host cells, *Mol. Microbiol. 52*, 631−641.
40. Raibaud, S., Schwarz-Linek, U., Kim, J. H., Jenkins, H. T., Baines, E. R., Gurusiddappa, S., Hook, M., and Potts, J. R. (2005) *Borrelia burgdorfery* binds fibronectin through a tandem b-zipper, a common mechanism of fibronectin binding in Staphylococci, Streptococci, and Spirochetes, *J. Biol. Chem. 280*, 18803−18809.
41. Schwarz-Linek, U., Hook, M., and Potts, J. R. (2006) Fibronectin-binding proteins of Gram-positive cocci. The molecular basis of fibronectin-mediated bacterial adherence to host cells, *Microbes Infect. 8*, 2291−2298.
42. Pilka, E. S., Werner, J. M., Schwarz-Linek, U., Picford, A. R., Meenan, N. A. G., Campbell, I. D., and Potts, J. R. (2006) Structural insight into binding of *Staphylococcus aureus* to human fibronectin, *FEBS Lett. 580*, 273−277.
43. Clark, R. A., Wikner, N. E., Doherty, D. E., and Norris, D. A. (1988) Cryptic chemotactic activity of fibronectin for human monocytes resides in the 120-kDa fibroblastic cell-binding fragment, *J. Biol. Chem. 263*, 12115−12123.
44. Ugarova, T. P., Zamarron, C., Veklich, Y., Bowditch, R. D., Ginsberg, M. H., Weisel, J. W., and Plow, E. F. (1995) Conformational transitions in the cell binding domain of fibronectin, *Biochemistry 34*, 4457−4466.
45. Ingham, K. C., Brew, S. A., and Erickson, H. P. (2004) Localization of a cryptic binding site for tenascin on fibronectin, *J. Biol. Chem. 279*, 28132−28135.

BI7001373